Academic Journal of Science and Technology
ISSN: 2771-3032 | Vol. 2, No. 1, 2022

A Design of an Equalized Gaussian Beam Antenna Applied in A Coal Mine Environment

Tianyuan Chen*, Lingfei Cheng, Ankang Liu

College of Physics and Electronic Information, Henan University of Science and Technology, Henan, China
* Corresponding author: Chen Tianyuan (Email: 786557005@qq.com)

Abstract: The environment of confined spaces such as tunnels and coal mines is complex and changeable. When the wireless signal propagates in it, it will be affected by the reflection and diffraction of the shaft wall, which puts forward higher requirements for the radiation beam of the coal mine antenna. In this paper, the corrugated horn antenna model is selected to design a coal mine antenna whose radiation pattern is almost equal to the Gaussian beam. Starting from the expression of Gaussian beam, combined with the radiation field formula of the horn antenna, the effects of slot depth, slot spacing, slot width and horn opening angle on the radiation beam are analyzed. The axial slot corrugated conical horn antenna designed in this paper has a gain greater than 13dBi in the frequency band, the side lobe level is less than -25dB, and the VSWR is less than 1.25 in the designed full frequency band. By comparing the pattern of the horn antenna and the pattern of the Gaussian beam, the results show that the axially grooved corrugated conical horn designed in this paper basically coincides with the Gaussian beam under ideal conditions, and the E and H planes are the Gaussian with a -10dB taper angle of 35°. The beams are basically the same. The equalized Gaussian beam antenna designed in this paper has important guiding significance for the antenna design in coal mine detection and exploration.

Keywords: Mine, Gaussian beam, Antenna, Wireless communication system.

1. Introduction

Coal is one of the important energy sources in China, and coal mining in China is mainly underground. In mine tunnels, wireless communication is an important means of communication to ensure production operation and personnel safety. [1-2] Underground tunnel environment is complex and harsh, the space is small, resulting in radio waves in the restricted space presents complex propagation characteristics, and the ground radio wave propagation characteristics are very different, resulting in the ground mature wireless communication system is difficult to smoothly transplant to the underground.[3-5] As the source end of the wireless communication system, the performance of the antenna has an important impact on the coverage effect of electromagnetic waves in mine tunnels.

The special environment of coal mine shaft, with serious multipath undulation, large wireless fading, and electromagnetic waves propagating in the restricted space on all sides, existing wireless communication is hardly applicable to underground communication. In order to solve the problem of restricted radiation beam in restricted space, scholars at home and abroad have conducted a lot of experiments and researches on this issue. The literature [6] shows that the signal attenuation rate of horizontally polarized antenna is smaller at the sidewall than at the top arm using geometric optical model simulation. The research team from China University of Mining and Technology discussed the effects of waveguide structure [7], dielectric wall electrical parameters, carrier frequency and wave propagation distance in the literature, and gave the optimal beam index for mining antennas. The literature [8] combines geometrical-optical theory and numerical method to give the calculation formula for the attenuation of electromagnetic transmission in the restricted space of electromagnetic wave coal mine. The Perceptive Mine Research Center of China University of Mining and Technology uses a model based on dielectric waveguide theory to derive the coupling efficiency and direction function of the antenna in the roadway. And the effect of the antenna location in the coal mine shaft on the radiation field distribution is simulated and analyzed with a horizontally polarized half-wave dipole as an example. [9] According to the geometry characteristics of the tunnel, Prof. Zhang Zhijun [10~12] believes that the mining antenna should have the characteristics of high gain and bi-directional radiation; Prof. Wang Junhong's [13] team uses ideal Gaussian beam as the simulation of transmitting antenna beam and studies the influence of parameters such as flap width, beam pointing, polarization mode and antenna position on the radio wave coverage in the tunnel. Most scholars do not give a better antenna solution [14~17] for the various problems that exist, so there is an urgent need for an antenna whose radiation beam can be better applied to the communication in the coal mine shaft.

This paper starts from the expression of radiation field of horn antenna and gives the theoretical model applicable to radiation beam in coal mine environment. On this basis, the corrugated horn antenna with high overlap with Gaussian beam is designed, and the main flap is obvious in the working band, and the sub-flap level is less than -25dB in both E-plane and H-plane, with excellent in-band matching characteristics.

2. Design Principle

The corrugated horn has outstanding advantages over the traditional light wall horn. Its directional diagram of each radiation plane has an almost complete equalization effect, and it has approximately coincident phase centers in the E plane and the H plane. Although the processing of corrugated horn is complicated, it is widely used in high-precision single pulse tracking, reflective surface antenna and other equipment due to its good electrical performance. The corrugated horn is made by embedding a corrugated groove in the conventional

light wall horn, which regulates the radiation field by suppressing the harmful electric field bypassing and deeply proportioning the content of each operating mode. As a result, good electrical performance with low subflap, low cross-polarization, wide frequency band and high aperture utilization can be achieved.

The designed horn form is a corrugated horn with axial slotting. It has been widely used because of its relatively simple design. Analysis of the radiation field of the corrugated conical horn is very complicated, so the field of the corrugated circular waveguide aperture is analyzed. The mixed mode of Hmn mode and Emn mode can be transmitted within the circular waveguide. By designing the slot depth d, slot width w, and tooth thickness t of the corrugated slot inside the waveguide, the operating modes are fully mixed and matched to transmit to the aperture surface to form the required field.

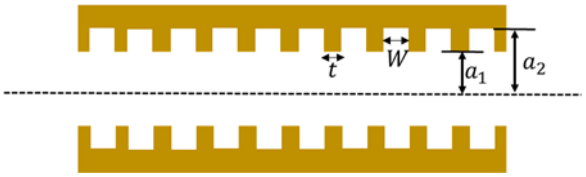

Figure 1. Corrugated circular waveguide

As shown in Figure 1, a polar coordinate system (ρ, φ) is established in the circular waveguide cross-section, and when the circular waveguide forms an equilibrium mixed-mode HE11 mode through the corrugated slot, then there is a circular waveguide caliber field distribution of the form

$$\begin{aligned}\overrightarrow{E_\rho}&=-jA_0J_0(k_c\rho)cos(m\varphi)\\ \overrightarrow{E_\varphi}&=jA_1J_0(k_c\rho)sin(m\varphi)\end{aligned} \tag{1}$$

in the formula $\gamma^2=k^2-k_c^2$, $J_0(k_c\rho)$ is the first type of Bessel function A1 is each normalization constant. Also transforming equation (1) into the right angle coordinate system, we have.

$$\begin{aligned}E_{xs}&=-jA_l\frac{\gamma}{k_c}J_0(k_c\rho)\\ E_{ys}&=0\end{aligned} \tag{2}$$

From (2), it can be learned that the aperture field is independent of the φ direction and is a circularly symmetric field. Far-field integration of the aperture field can be obtained as a function of the radiation direction of the waveguide radiator. The principle of the corrugated horn is similar to that of the corrugated waveguide, both of which use the slot spacing and slot depth to change the working mode to form an equilibrium mixed mode, which is finally integrated on the aperture surface.

The Gaussian beam can be approximated as a conical beam of a horn antenna, and there is no sub-flap or cross-polarization in any direction, which can be used for point-to-point communication in restricted spaces such as coal mines. The Gaussian beam is composed of an electric dipole along the x-axis placed at the complex space position (0, 0, jb) and a magnetic dipole along the y-axis placed at the complex space position (0, 0, -jb), after deducing that it produces a radiation field of

$$\vec{E}(r,\theta,\varphi)=A\frac{e^{-jkr}}{kr}e^{kbcos\theta}(1+cos\theta)\left(cos\varphi\vec{\theta}-sin\varphi\vec{\varphi}\right) \tag{3}$$

where (r, θ, φ), is the spherical coordinate system in which the Gaussian beam is located, and A is a constant.

From equation (3), the Gaussian beam can be varied by changing the coordinates of its position b placed in complex space to change the level AdB at a given angle θ. The relationship is

$$b=\frac{20lg\left(\frac{1+cos\theta}{2}\right)-A}{20k(1-cos\theta)lg\,e} \tag{4}$$

2.1. Antenna Design and Simulation

As shown in Figure 2, the design structure of corrugated cone horn is generally divided into four segments, namely, radius transformation segment, mode transformation segment, transition segment and radiation segment. Firstly, the functions and design principles of each segment are introduced; among them, the mode transformation segment is used to generate HE11 mode and adjust the mode ratio of EH12 and HE11 to eliminate cross-polarization. Transition section and radiation section to achieve tensor transformation, change the radiation direction map of the cone cutting. The radius conversion section is used to achieve impedance matching with the first three sections of the structure, reduce return loss and achieve better impedance matching.

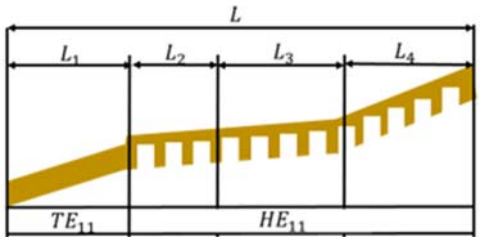

Figure 2. General structure of corrugated horn

The design of the transform section can be a linear model or a curved model, and the linear section length L1 can be determined by parametric scanning to achieve impedance matching. The mode transformation section can be determined by the desired frequency band, the slot depth is generally transformed by λ/4~λ/2, and the number of open slots is generally 4 slots per wavelength. The slot depth of the final transition section and radiation section is about λ/4, and the tensor angle is determined by the required design cone cutting index.

In order to prevent the transmission of higher modes, the input radius R of the circular waveguide is taken to be

$$\frac{\lambda}{3.41}\le R\le\frac{\lambda}{2.62} \tag{5}$$

However, since the structure of symmetric structure will not transmit the mode of asymmetric structure, the circular waveguide cannot produce the mode with m > 1 and the optimal transmission radius of HE11 mode is

$$r=\frac{\lambda}{1.843} \tag{6}$$

The radius conversion section and the mode conversion

section are combined into one, which is a stepped axial corrugated slot structure. As shown in Fig. 4(c), where: d1 is the corrugated horn length; d2 is the length of the moment circle conversion section; R is the outer diameter of the horn aperture; R0 is the inner diameter of the horn aperture; r1 is the outer diameter of the circular waveguide aperture; r2 is the inner diameter of the circular waveguide aperture; dt is the circular waveguide wall thickness; w is the width of the corrugated slot; t is the thickness of the corrugated slot teeth; A to D are the slot depths of each section of the corrugated slot, respectively; a is the wide edge of the rectangular waveguide; b is the rectangular waveguide narrow edge.

The slot pitch is generally taken as λ/10~λ/5. And the tooth thickness should be as much as possible under general circumstances, but the smaller the tooth thickness is, the more difficult it is to process and the bigger the error is. So the tooth thickness is generally 0.1-0.3 times the slot spacing. The slot depth is used to adjust the mode content ratio and suppress the harmful current, so the slot depth at the aperture is about equal to λ/4. And the slot depth at the horn neck is about equal to λ/2, which is used for mode transformation and adjustment. Finally, the radiation radius R0 of the horn antenna, which is used to adjust the width of the directional map.

Since the actual engineering will not feed directly to the circular waveguide, a moment-circle conversion section is added, as shown in Figure 3. The rectangular waveguide is designed to excite a mode similar to the main mode of the circular waveguide. The long side of the rectangular waveguide in this mode is generally between λ/2 and λ, and the wide side is generally λ/4.4 to λ/2.2.

Figure 3. Schematic diagram of the structure of the rectangular-circle conversion section

2.1.1. Simulation of Corrugated Cone Horn

The design target gain of the Gaussian-like beam antenna applied to coal mine environment is >13dBi, -10dB cone clipping angle: 34°~36°, VSWR<1.5 in bandwidth; according to the above design requirements, the feed source is simulated and analyzed in HFSS software. The corrugated cone horn model and outer dimensions are shown in Figure 4.

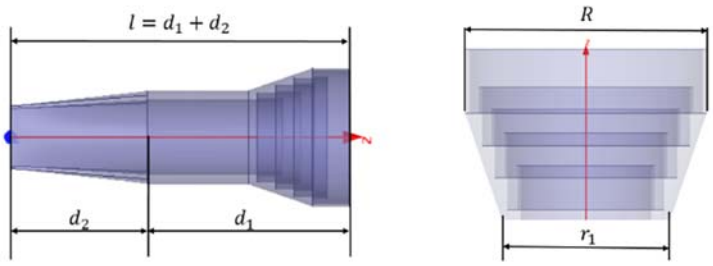

(a) Corrugated horn outer dimensions

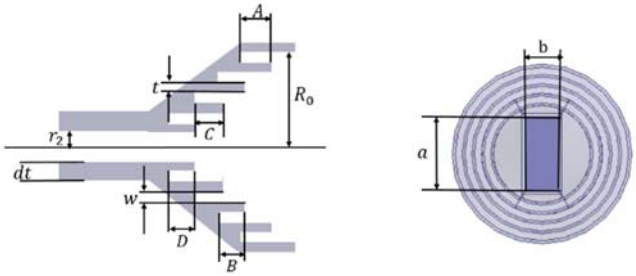

(b) Corrugated horn inner dimensions and conversion section dimensions

Figure 4. Corrugated horn model

Table 1. Parameter of the simulation

Parameters	Meaning
d_1	Corrugated horn length
d_2	Length of moment circle conversion
R	Outside diameter of horn caliber
R_0	Inner diameter of horn bore
r_1	Outer diameter of circular waveguide
r_2	Inner diameter of circular waveguide
dt	Circular waveguide wall thickness
w	Corrugated groove width
t	Corrugated groove tooth thickness
A~D	Depth of each section of corrugated
a	Rectangular waveguide broadside
b	Rectangular waveguide with narrow

In order to obtain the expected gain index and achieve a usable Gaussian-like beam, the minimum caliber 2R0 of the horn can be calculated for the caliber field is 45.52 mm (assuming 100% utilization of the horn caliber). The design range of calculated aperture and slot width is

$$\begin{aligned} &r_2 + 4(w+t) > 22.76mm \\ &9.32mm < r_2 < 12.21mm \end{aligned} \tag{7}$$

As shown in Figure 5, the beam width of the horn widens with the increase of r2 when other parameters are certain. Therefore, the inner radius of the waveguide is taken to be 12mm, and the circular waveguide will not produce high secondary modes at this radius.

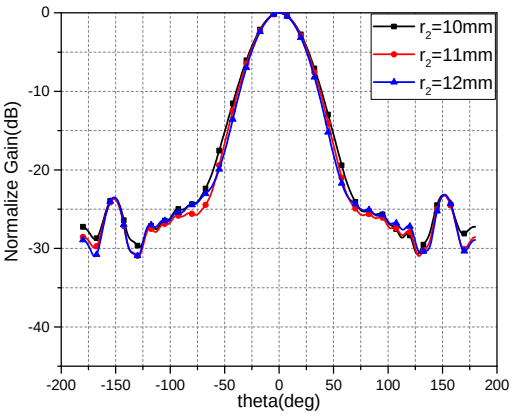

(a) Effect of circular waveguide inner diameter on horn E surface

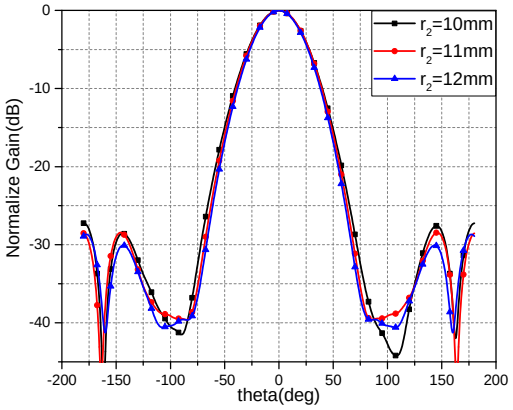

(b) Effect of circular waveguide inner diameter on the H surface of the horn

Figure 5. Effect of the inner radius of the circular waveguide on the directional map of the horn

After the radius size inside the circular waveguide segment is selected, the flap width of the horn can be adjusted by changing the slot width. It is known that when the radius of circular waveguide is 12mm and the slot depth is 8mm (λ/4), the minimum slot width determined by equation (7) is 2.92mm. The horn -10dB cone cutting angle is about 43° at this time. In order to reduce the corrugated horn beam width, the slot width needs to be expanded appropriately.

The final design of the corrugated cone horn dimensions are shown in Table 2.

Table 2. Parameter of the horn

Parameters	Size
d_1	88mm
d_2	60mm
a	25mm
b	11.4mm
w	3mm
t	0.5mm
r_2	12mm
A	8mm
B	8mm
C	8mm
D	8mm
R_0	26mm

The results obtained by modeling and simulating in HFSS according to this dimension are shown in Figure 6(a). Figure 6(b) shows the comparison of the designed horn E-plane directional diagram and the ideal Gaussian beam with the -10dB taper angle of the Gaussian beam of 35°. The E-plane directional diagram of horn No. 1 in the figure is basically equalized with the H-plane directional diagram. Although the directional diagram in the E-plane basically overlaps with the ideal Gaussian beam, its sub-flap and post-flap are electrically averaged greater than -30 dB.

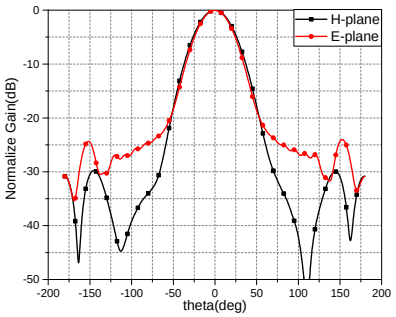

(a). Radiation direction diagram of No.1 horn

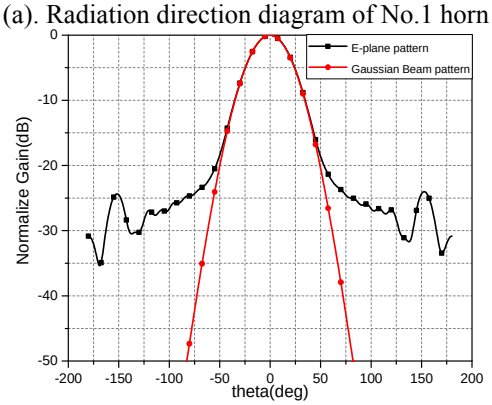

(b). Comparison of the E-plane of horn No. 1 with the ideal Gaussian beam

Figure 6. Horn Antenna radiation direction diagram simulation results

This horn causes problems such as severe asymmetry in the directional map and shifted beam pointing when communicating in the narrow space of a coal mine shaft. Therefore, there is a need to improve the sub-flap, post-flap level and cone chipping distribution of the horn. From the aforementioned theory, it is known that the corrugated slot can suppress the E-plane bypass current and make the E-plane directional map close to the H-plane directional map. As shown in Figure 11, decreasing the depth of the corrugated slot A will reduce the E-plane subvalve level, and increasing the depth of the corrugated slot B will reduce the E-plane subvalve level. Increasing the depth of ripple slot C reduces the E-side flap level, and increasing the depth of ripple slot D reduces the taper angle. Determine the depth of each slot to reduce the subvalve and readjust the circular waveguide inner diameter and slot width.

2.2. Simulation 2

The voltage standing wave ratio in the band of the final optimized horn is shown in Figure 7(d), and it can be seen that VSWR <1.25 can be achieved in the bandwidth. the equalization characteristics in the band of the improved corrugated horn are good, and the -3dB beamwidth and -10dB beamwidth of the E and H planes of each frequency point are approximately equal, with good consistency. The radiation direction diagram of each frequency point is shown in Figure 7 (a), (b) and (c), in which the main flap of the radiation direction diagram of each frequency point is sharp, and the

direction diagram of E and H surfaces of each frequency point is highly consistent, with good equalized Gaussian beam shape.

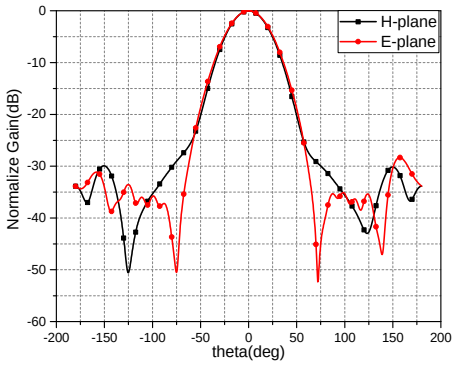

(a) 9.27GHz frequency horn direction diagram

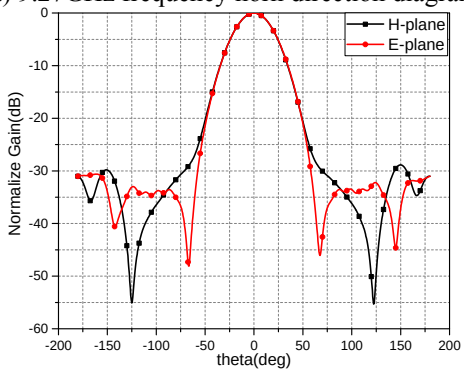

(b) 9.37GHz frequency horn direction diagram

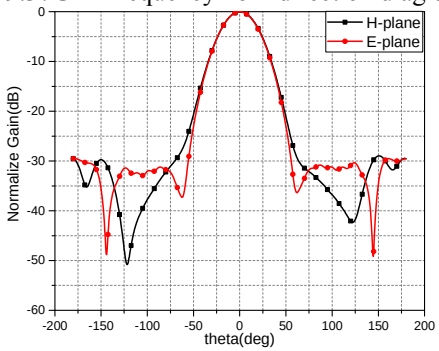

(c) 9.47GHz frequency horn direction diagram

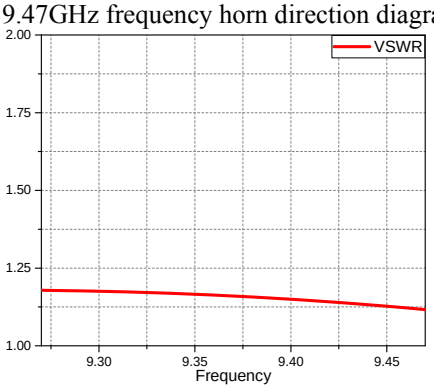

(d) Voltage VSWR in the horn band

Figure 7. Corrugated Horn Simulation Results for Improved Design

The results show that the sub-flap and post-flap levels of the improved design horn are significantly lower and have a better overlap with the Gaussian beam.

3. Conclusion

The corrugated horn antenna suppresses the horn mouth-plane bypass current through the corrugated slot, and transmits the approximately circularly symmetric HE11 pattern using the corrugated slot. This paper briefly introduces the derivation process of the corrugated horn antenna mouth surface field as well as the radiation field. The design principles of the axial slot corrugated conical horn are highlighted, including the selection of slot depth, slot spacing, slot width, and horn tension angle. The axial slotted corrugated conical horn antenna designed in this paper has a gain of more than 13dBi in the frequency band, the subflap level is less than -25dB, and the VSWR is <1.25 in the full band range of the design. the results of the comparison between the directional diagram of the horn antenna and the directional diagram of the Gaussian beam show that the axial slotted corrugated conical horn designed in this paper has good electrical performance with the basic coincidence of the Gaussian beam under ideal conditions.

Acknowledgment

We thank Prof. Lingfei Cheng and Chen Nuo for their support, and this work was supported by a project grant from the School of Physics and Electricity of Henan University of Technology.

References

[1] Forooshani A E , Bashir S , Michelson D G , et al. A Survey of Wireless Communications and Propagation Modeling in Underground Mines[J]. IEEE Communications Surveys & Tutorials, 2013, 15(4):1524-1545.

[2] Large D , Ball L , Farstad A . Radio Transmission to and from Underground Coal Mines--Theory and Measurement[J]. IEEE Transactions on Communications, 1973, 21(3):194-202.

[3] Hu QS, Zhang SH, Wu LX, et al. Mine dynamic targeting:challenges, status and trends[J]. Journal of Coal, 2016(5 issues):1059-1068.

[4] Dudley D , Lienard M , Mahmoud S , et al. Wireless propagation in tunnels[J]. IEEE Antennas and Propagation Magazine, 2007, 49(2):11-26.

[5] Wang Jun, Li Shaoqian, WANGJun, et al. Cognitive radio: principles, technologies and development trends[J]. ZTE Communication Technology, 2007, 13(3):27-31.

[6] Y. Huo, Z. Xu, H. Zheng and X. Zhou, "Effect of antenna on propagation characteristics of electromagnetic waves in tunnel environments," 2009 Asia Pacific Conference on Postgraduate Research in Microelectronics & Electronics (PrimeAsia), Shanghai, China, 2009, pp. 268-271.

[7] Huo Yu,Zheng Hongdang,Hu Yanjun,Zhang Guopeng. Optimal beam indicators of mining antennas for application in rectangular roadways[J]. Journal of Coal,2017,42(10):2776-2782.

[8] Zhang Yanwei. Study on the transmission characteristics of electromagnetic waves in restricted spaces under mines[D]. Supervisor: Zhang Jilong. North Central University,2009.

[9] Huo Yu,Liu Fengxue,Xu Zhao. Influence of mine shaft antenna location on radiation field distribution[J]. Journal of Coal,2013,38(04):715-720.

[10] Liu L , Zhang Z , Tian Z , et al. A Bidirectional Endfire Array With Compact Antenna Elements for Coal Mine/Tunnel Communication[J]. IEEE Antennas and Wireless Propagation Letters, 2012, 11:342-345.

[11] Liu W , Zhang Z , Tian Z , et al. A Bidirectional High-Gain Cascaded Ring Antenna for Communication in Coal Mine[J]. IEEE Antennas and Wireless Propagation Letters, 2013, 12:761-764.

[12] Li Dawei. Research on the Characteristics of Radio Wave Coverage in Restricted Spaces [D]. 2016.

[13] Shaikh A E , Majeed F , Zeeshan M , et al. Efficient implementation of deterministic 3-D Ray Tracing model to predict propagation losses in indoor environments[C]// Personal, Indoor and Mobile Radio Communications, 2002. The 13th IEEE International Symposium on. IEEE, 2002.

[14] Choudhury B , Jha R M . A refined ray tracing approach for wireless communications inside underground mines and metrorail tunnels[C]// Applied Electromagnetics Conference (AEMC), 2011 IEEE. IEEE, 2011.

[15] Chen S H , Jeng S K . SBR image approach for radio wave propagation in tunnels with and without traffic[J]. IEEE Transactions on Vehicular Technology, 1996, 45(3):570-578.

[16] Hrovat A, Kandus G, Javornik T. Four-slope channel model for path loss prediction in tunnels at 400 MHz[J]. IET Microwaves, Antennas & Propagation, 2010, 4(05):571-582.

[17] Cheng Lingfei. Equivalent analysis method of electromagnetic wave propagation in semi-circular arched roadway[J]. Journal of Henan University of Science and Technology (Natural Science Edition), 2007(05):72-76.